А С Т Р О Ф И З И К А

ТОМ 64 МАЙ, 2021 ВЫПУСК 2

MODULATION OF GALACTIC COSMIC RAYS DUE TO MAGNETIC CLOUDS AND ASSOCIATED STRUCTURES IN THE INTERPLANETARY SPACE: 1996-2018

M.FADAAQ, B.BADRUDDIN

Recieved 27 February 2021
Accepted 3 May 2021

We study the modulation of galactic cosmic rays due to magnetic clouds observed during solar cycles 23 and 24 (1996-2018). We utilize solar wind plasma and field data together with cosmic ray intensity (CRI) data during the passage of magnetic clouds and associated structures. We apply superposed epoch analysis to analyze these data. We study the relative importance of magnetic clouds and their associated structures in modulating the cosmic rays. We observe significant differences in the amplitudes and time profiles of transient depressions in cosmic ray intensity due to magnetic regimes of different field strengths and topologies. We discuss the observed results in light of differences in the simultaneous plasma and magnetic field properties.

Keywords: *cosmic ray: interplanetary space: magnetic cloud: solar wind: interplanetary magnetic field*

1. *Introduction*. Magnetic clouds are high-field structures propagating in the interplanetary space. They are a subset of interplanetary coronal mass ejection (ICME) characterized by the high magnetic field, low proton temperature, low plasma beta, and smoothly rotating magnetic field [1,2]. ICMEs can significantly affect near-Earth space, geomagnetic activity [3-7] and galactic cosmic ray (GCR) intensity [8-20] in the interplanetary space, especially when they are driving shock and forming shock-sheath region ahead [21-24].

Moreover, there is some evidence that magnetic clouds (MC) structures are more geo-effective (i.e., effective in producing geomagnetic disturbances) as well GCR-effective (i.e., effective in depressing the GCR intensity) than the ICME structures that are not magnetic clouds [25-27].

In this work, we concentrate specifically on the role of MCs and their associated feature in transient GCR-modulation using a large set of MC data for the last two solar cycles 23 and 24. These MCs provide an exciting set of interplanetary structures. Some of them are just high-field closed magnetic structures with specific field topology (isolated MCs). Some of these closed high field structures are followed by high-speed solar (HSS) wind streams, presumably from the open field region of coronal holes (MCs followed by HSS). In addition, many other MCs are associated with a shock-sheath region preceding them (shock-associated MCs). The shock-sheath region forms ahead of an MC due to the interaction between high-speed MCs and slower ambient solar wind plasma and magnetic field. The magnetic field is high both in the MC and the shock-sheath region. However, in contrast to the smooth and closed magnetic field (flux rope) inside the MC, the magnetic field in the shock-sheath region is usually turbulent [11,28,29]. Thus, by studying the effectiveness of these high magnetic field regions with different field properties and topologies, we can isolate the magnetic regime most important for transient cosmic ray modulation. Consequently, we can identify physical mechanisms playing an important role in the transient modulation of cosmic rays.

Forbush decreases (sudden decreases in GCR intensity within about a day followed by a slower recovery of intensity in few days) play an important role in transient modulation of GCRs. Such depression is often observed during the passage of shock-sheath-associated magnetic clouds. However, the role of the turbulent magnetic field (in shock-sheath region) and smooth magnetic field (in MCs), their relative contribution in generating Forbush decreases has been debated for quite some time [22,28,30] after their identification from space observations [1]. The relative contribution of the shock-sheath and MC regions to Forbush decreases has generally been inconclusive. It ranges from essentially no role of MCs [22,28,31] to some minor role [11,22] or even equal role [25] of MCs in transient modulation of GCRs due to shock-associated magnetic clouds. In this work, we intend to focus our study on the following points: (a) whether an isolated MC, without any additional associated feature preceding or following it, is effective in transient modulation of cosmic rays, (b) does a high-speed solar wind stream (HSSWS) following a magnetic cloud has any significant influence in modulating the cosmic ray intensity, and (c) what is the relative importance of shock-sheath and magnetic cloud regions of different field properties in transient modulation of cosmic rays. This work aims to provide further insight into the phenomenon of transient Forbush decreases after performing a systematic study using magnetic clouds with different associated features detected during solar cycles 23 and 24.

2. *Data and analysis*. We have utilized the magnetic clouds observed in the near-Earth space for two consecutive solar cycles 23 and 24 (1996-2018) [http://www.srl.caltech.edu/ACE/ASC/DATA/level3/icmetable2.htm]. Neutron monitor data of two stations, Oulu [https://cosmicrays.oulu.fi/] and Moscow [http://cr0.izmiran.ru/mosc/main.htm] were used as a measure of galactic cosmic ray intensity. Interplanetary plasma and field data [https://omniweb.gsfc.nasa.gov/form/dx1.html] were also utilized. In this work, hourly data of GCR intensity and interplanetary plasma and field parameters were subjected to superposed epoch

analysis with respect to MCs of different specified groups, detected during continuous 23 years spanning two recent solar cycles 23 and 24. For the data analysis, all the detected MCs were divided into three groups: (A) In this group of magnetic clouds, the solar wind disturbances (sudden enhancement in solar wind plasma velocity, plasma density, temperature, and pressure, as well as an interplanetary magnetic field) were observed a few hours before the MC arrival (shock-associated magnetic clouds). (B) In this group of MCs, no disturbance in plasma and field parameters is detected ahead of MCs, but they were followed by the high-speed solar wind. (C) This group of MCs was just the high magnetic field structures of magnetic clouds without any disturbance before or after it.

Cosmic ray and plasma/field data were analyzed using superposed epoch analysis, with reference to all the above groups of MCs. For the analysis of cosmic ray, plasma, and field data during the passage of group (A) magnetic clouds (i.e., shock-sheath associated MCs), the epochs were systematically shifted as (i) start time of shock (ii) start time of MC, (iii) time of maximum magnetic field strength and (iv) time of maximum sigma in magnetic field vector (SigmaF) during the passage of shock-sheath-MC structure. Superposed Epoch analysis of neutron monitor, and solar wind plasma and field data has also been performed with respect to the arrival time of MCs (not associated with shock-sheath region), both followed (group B) and not followed (group C) by high-speed solar wind streams presumably originating in coronal holes.

In addition to superposed epoch analysis, correlation analysis has also been performed between the magnitude of cosmic ray decrease due to the passage of individual MCs and corresponding magnitudes of various solar wind plasma and field parameters and their functions.

3. *Results and discussion*. A magnetic cloud moving in interplanetary space, if fast enough, forms a shock-sheath region ahead of it due to its interaction with the slower ambient solar wind plasma and interplanetary magnetic field. Thus, a unified structure (shock-sheath-MC) may pass a point in space (e.g., Earth/spacecraft) during its propagation into the interplanetary space. At the time of shock crossing, there is a sudden jump in the plasma parameters (solar plasma velocity, density, and temperature) and the interplanetary magnetic field strength. Plasma density and temperature remain enhanced during the passage of the sheath region (sheath duration is usually $\lesssim 1$ day), while these interplanetary plasma parameters are much lower during the passage of MC. On the other hand, the magnetic field strength remains enhanced both during the passage of the shock-sheath and MC region. However, although enhanced, the magnetic field within the shock-sheath region is turbulent. It is magnetically quit (non-turbulent) with smooth field lines inside the MC [28,32].

However, slow MCs propagating in interplanetary space with nearly the same speed as the ambient solar wind are unlikely to form a shock-sheath region in front of them. Such MCs are a low density, the low-temperature region of the high magnetic field with specific field topology. We call them MCs not associated with shock or MCs without shock.

In Fig.1a, we have plotted the superposed epoch analysis results of hourly data of cosmic ray intensity together with interplanetary plasma and field data. Cosmic ray intensity data from two neutron monitoring stations, Oulu and Moscow, are plotted in this figure. Interplanetary plasma and field data plotted in this figure are: Solar wind velocity V, Interplanetary magnetic field (IMF) strength B, its north-south component Bz, Sigma in IMF vector σF, "Normalized σF" $\sigma F/B$, and Interplanetary electric field BV/1000.

The superposed epoch plots have been generated using these data from 3 days (72 hours) before the epoch (zero hour) till nine days (216 hours) after the epoch time. In this Fig.1a, the epoch time is the start time (arrival) of shock disturbance of the shock-associated magnetic cloud crossing the near-Earth space observed during 1996-2018. This figure provides the plasma, field, and cosmic-ray behavior for three days before the arrival of shock-associated MCs, at the shock time, during the passage of the sheath region, during magnetic clouds, and up to several days after the passage of shock-sheath-MC structures. Simultaneous plots of neutron monitor data provide cosmic-ray behavior before, during, and after the passage of such structures. The selected plasma and field parameters enable us to identify, and distinguish between, the shock-sheath-MC structures and/or help us in understanding the physical mechanism of transient modulation of galactic cosmic rays.

Fig.1a provides the average cosmic ray response to the passage of shock-associated MC of two solar cycles (23 & 24), in addition to useful information about plasma and field properties during the passage of distinct regions of the structure. Examination of Fig.1a shows that the GCR intensity started decreasing near the zero hour (arrival of shock); it reached a minimum intensity level in two steps. The first step (~85% of total decrease) happens within the first few (~8) hours. During the second step, the slower one ~15% of the total decrease occurs in ~16 hours. Thus, the total average duration of intensity decrease being ~24 hours. After reaching a minimum level, the intensity starts increasing (recovering), and complete recovery to the pre-decrease level takes several days.

From the average pattern of variations/changes in the GCR intensity and interplanetary plasma/field parameters before, during, and after the passage of shock-sheath-MC structure, we observe the following (see Fig.1a). A sudden increase in parameters B, V, σF, $\sigma F/B$, and BV/1000 indicates the arrival of shock front of the shock-sheath-MC structure. Almost at the same time, we notice a fast decrease in GCR intensity at both the neutron monitors at Oulu and

Moscow.

The whole intensity decrease (start till minimum) appears to proceed in two steps. The first and faster step of decrease occurs during the first few hours of the passage of the high magnetic region. During this short period, σF is quite high (~2-3 times the ambient value), and "normalized σF" (i.e., $\sigma F/B$) remains higher than its ambient value.

Considering the duration of enhanced "normalized σF ($\sigma F/B$)" above its normal (ambient) value as the duration of sheath passage, and below normal value as the duration of magnetic cloud, the first and faster step of GCR intensity decrease happens during the passage of sheath region.

After the passage of the sheath region, the GCR intensity decreases at a slower

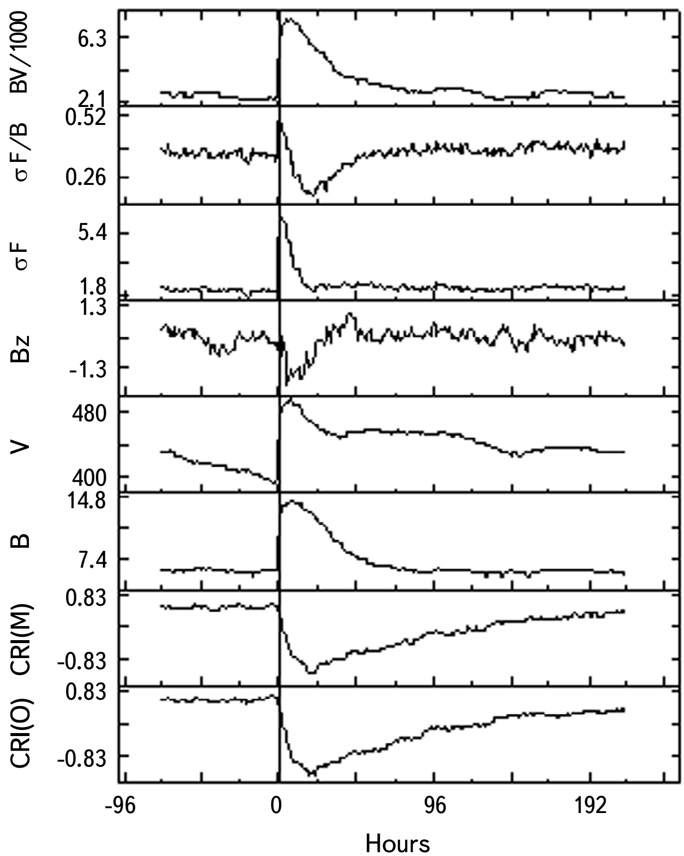

Fig.1a. Superposed epoch analysis results of hourly neutron monitor data of Oulu [CRI(O) (%)] and Moscow [CRI(M) (%)] stations, magnetic field [B (nT)], solar wind velocity [V (km s^{-1})], north-south component of magnetic field [Bz (nT)], sigma in magnetic field vector [Sigma F(nT)], normalized Sigma F [SigmaF/B] and interplanetary electric field [BV/1000 (mV/m)] during the passage of shock-associated magnetic clouds observed in solar cycle 23&24 (1996-2018); Epoch (zero time) corresponds to start time of shock.

rate and the intensity reaches its lowest level after a few hours. This minimum intensity level is interestingly observed at a time when the "normalized σF ($\sigma F/B$)" reaches its minimum level, σF again reaches its normal (ambient) level, and at the time of polarity reversal in the magnetic cloud. Thus, the intensity minimum during the passage of shock-sheath-MC structure appears to happen when the magnetic field variance in MC is at its minimum (lowest $\sigma F/B$) at the time of passage of central axis (time of polarity reversal).

Although the set of MCs used for this plot consists of MCs of all possible polarities, the average Bz behavior shows a southward to northward (SN) turning MC [1,32,33]. Considering the field rotation in the average polarity profile (SN polarity) and $\sigma F/B$ value returning to a normal level, the average duration of passage of the shock-sheath-MC structure can be taken as ~48 hours.

The GCR intensity starts recovering ~24 hours after the onset, suggesting that intensity starts recovering even when the MC structure has to cross the point of observation (e.g., Earth). The complete recovery takes several days even after the passage of MC and associated structure.

The parameter "normalized σF (i.e., $\sigma F/B$)" appears to be a good additional parameter in the identification of shock arrival, as well as in distinguishing between the sheath and MC durations during the passage of shock-sheath-MC structure [27].

To distinguish between the effect of shock-sheath and MC in transient modulation of GCR intensity, we performed the superposed epoch analysis of all the earlier utilized parameters in Fig.1a, but taking the epoch (zero hour) as the MC start time (see, Fig.1b). We observe from Fig.1b that the GCR intensity decrease starts earlier than the arrival of MCs in shock-associated MCs, and major parts of the decrease happen before the arrival of the MC. However, the minimum intensity is attained during the passage of the MC. This intensity minimum happens when $\sigma F/B$ is lowest, and Bz is highest (southward) in the MC. However, the intensity minimum occurs somewhat later than the time of highest field strength (B). The intensity starts increasing (recovering) even though the MC is still passing the observation point, as evident from the time profile plot of parameters B, Bz, and $\sigma F/B$.

In the past, studies have suggested that the amplitude of transient GCR intensity decrease is well correlated (inversely) with the strength of the magnetic field [25,27]. Thus, it will be interesting to see that whether the time of GCR intensity minimum also occurs at the same time as the maximum field intensity. For this purpose, we performed the superposed epoch analysis of the same set of data as in Fig.1a and Fig.1b, but the epoch shifted to the time of maximum field intensity in each shock-associated MC. We observe (see Fig.1c) that the GCR intensity minimum occurs not at the time of field maximum but several hours after the field maximum during the passage of shock-associated MCs.

We observed in Fig.1a that most of the GCR intensity decrease occurs during the passage of sheath, the region of high σF and $\sigma F/B$. There are some evidences [14] that the amplitude of σF may be correlated (inversely) with the magnitude of GCR intensity decrease during the passage of shock-associated coronal mass ejections. Thus, it seems prudent to see if the GCR intensity minimum occurs when σF is maximum during the passage of shock-associated MCs. For this proposed, we performed superposed epoch analysis of the same set of GCR-intensity and interplanetary plasma/field data as in Fig.1a, but the epoch shifted at the time of the maximum value of σF during the passage of each shock-

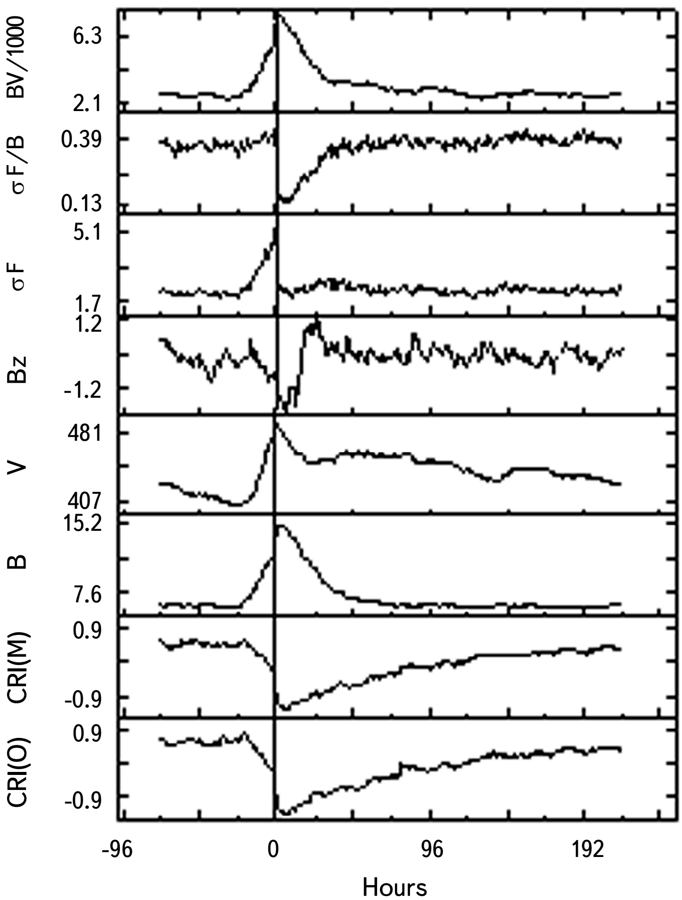

Fig.1b. Superposed epoch analysis results of hourly neutron monitor data of Oulu [CRI(O) (%)] and Moscow [CRI(M) (%)] stations, magnetic field [B (nT)], solar wind velocity [V ($km\,s^{-1}$)], north-south component of magnetic field [Bz (nT)], sigma in magnetic field vector [Sigma F(nT)], normalized Sigma F [Sigma F/B] and interplanetary electric field [BV/1000 (mV/m)] during the passage of shock-associated magnetic clouds observed in the solar cycle 23&24 (1996-2018); Epoch (zero time) corresponds to start time of MCs.

associated MCs (see Fig.1d). We observe that GCR intensity minimum does not occur at the same time as the σF maximum, but the time of intensity minimum lags by a few hours the time of σF maximum, during the passage of shock-associated MCs.

All the MCs, observed in near-Earth space are not associated with a shock-sheath region. Some of them are just the structures of high field strength with specific plasma and field properties [25,32]. Thus, it is important to know whether these high fields magnetically quiet structures can also produce a significant decrease in GCR intensity when they are not accompanied by a magnetically turbulent high field shock-sheath region. We have performed superposed epoch

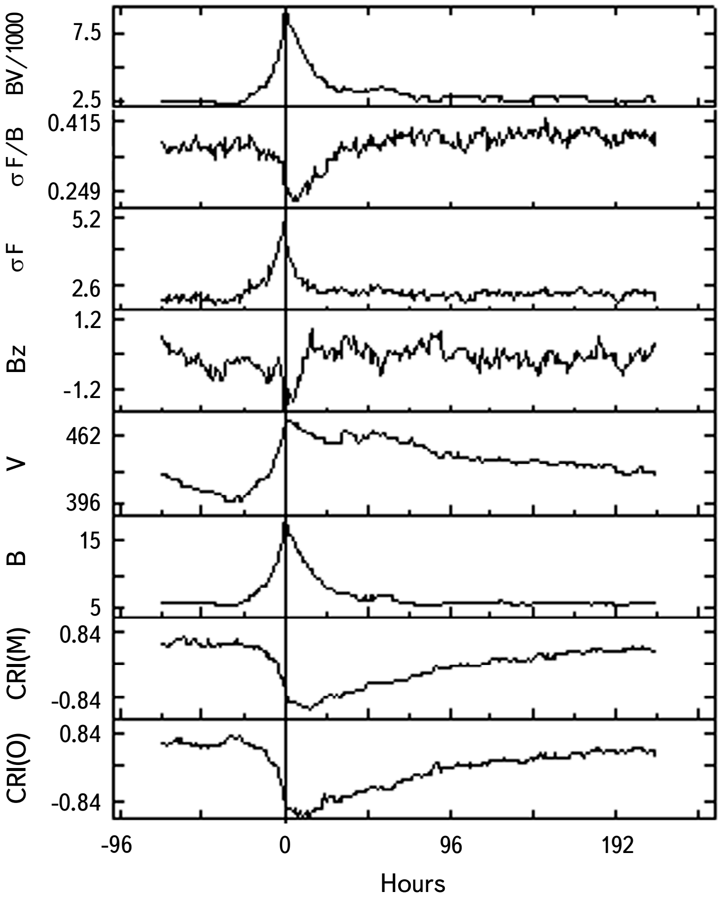

Fig.1c. Superposed epoch analysis results of hourly neutron monitor data of Oulu [CRI(O) (%)] and Moscow [CRI(M) (%)] stations, magnetic field [B (nT)], solar wind velocity [V ($km\,s^{-1}$)], north-south component of magnetic field [Bz (nT)], sigma in magnetic field vector [Sigma F (nT)], normalized Sigma F [Sigma F/B] and interplanetary electric field [BV/1000 (mV/m)] during the passage of shock-associated magnetic clouds observed in the solar cycle 23 & 24 (1996-2018); Epoch (zero time) corresponds to time of maximum field strength (B-max).

analysis of the same set of cosmic ray and solar wind plasma/field data (as in earlier plotted figures), with respect to the arrival time of MCs not-associated with shock. We observe (see Fig.2a) that passage of such structures does not produce Forbush-type decrease as observed in case of shock-associated MCs (e.g., Fig.1a).

Further, GCR intensity decrease during and after the passage of such MCs is slowly varying depression of small amplitude followed by a slow recovery (see Fig.2a). Such time profiles are generally observed during the passage of high-speed solar wing streams [14,34,35]. From the time profile of B and σF/B in this figure, it appears that the average duration of magnetic clouds is ~24 hours. A careful examination of Fig.2a shows that after MC passage, the cosmic ray intensity remains depressed for quite some time.

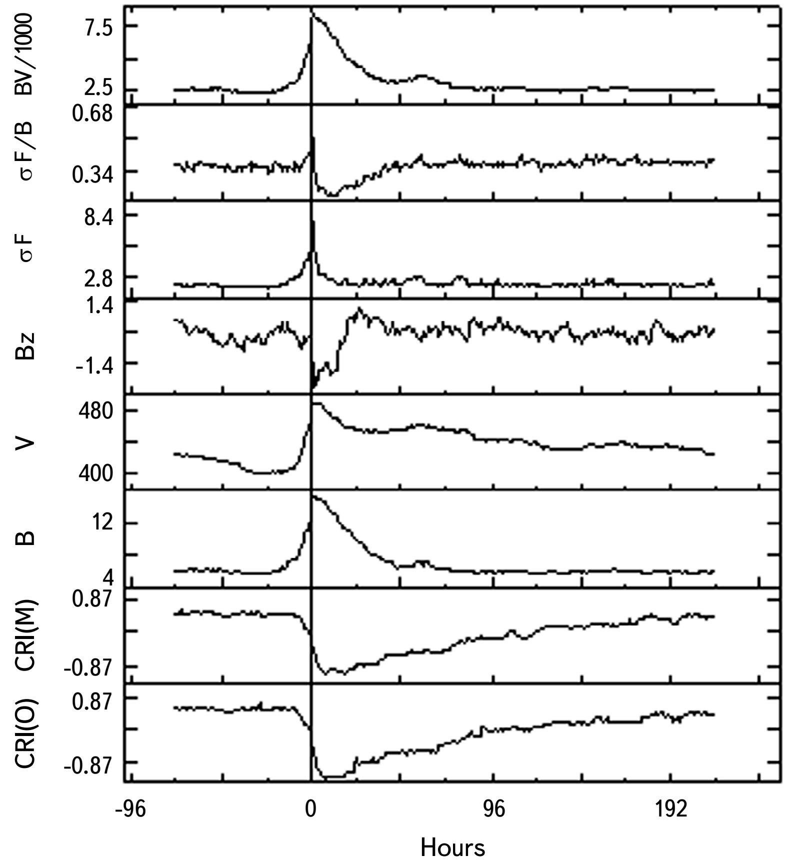

Fig.1d. Superposed epoch analysis results of hourly neutron monitor data of Oulu [CRI(O) (%)] and Moscow [CRI(M) (%)] stations, magnetic field [B (nT)], solar wind velocity [V (km s^{-1})], north-south component of magnetic field [Bz (nT)], sigma in magnetic field vector [Sigma F(nT)], normalized Sigma F [Sigma F/B] and interplanetary electric field [BV/1000 (mV/m)] during the passage of shock-associated magnetic clouds observed in the solar cycle 23&24 (1996-2018); Epoch (zero time) corresponds to time of σF maximum.

It is interesting to note from this figure that there is a significant enhancement in the solar wind velocity after the passage of MC. Thus, it is also a possibility that this enhanced solar wind speed after MC passage may also have influenced the cosmic ray intensity time profile [30,34,36].

In order to see whether this depression, although small, is due to MCs or it is influenced by enhanced solar wind speed following MCs not-associated with shocks, we divided this set of MC into two groups. One, those MCs followed by significant enhancement of solar wind velocity. Two, those MCs following which there is no enhancement in solar wind up to at least ~24 hours after their passage.

We performed the superposed epoch analysis of the same set of neutron monitor and interplanetary plasma/field data as in earlier figures, with epoch (zero hour) as the arrival time of MCs followed by the solar wind of high speed. We

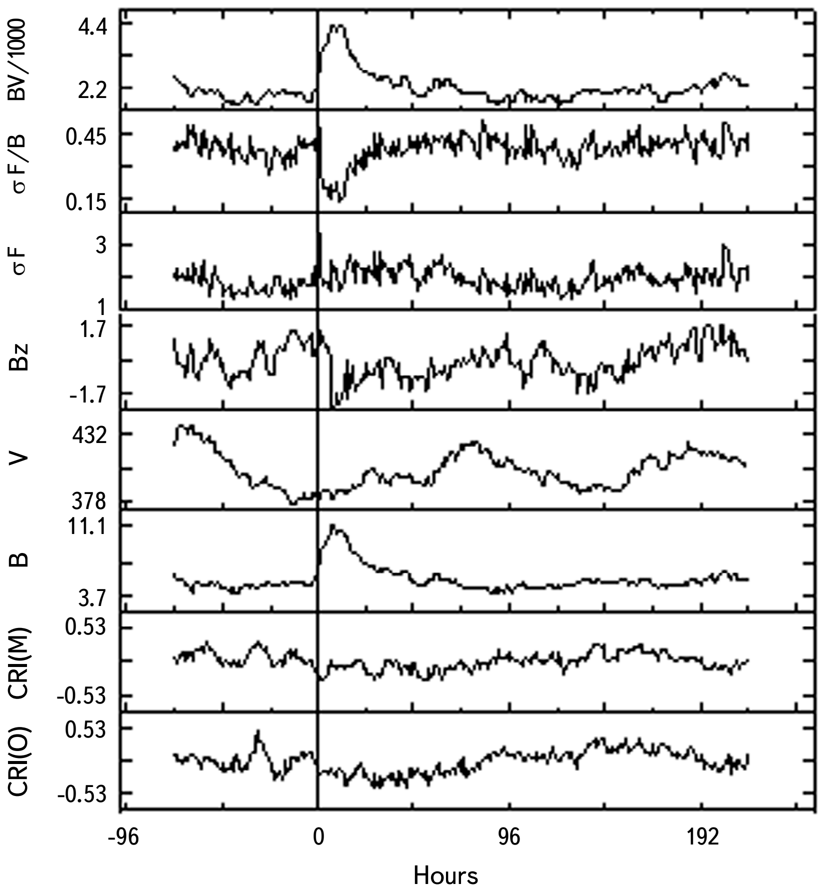

Fig.2a. Superposed epoch analysis results of cosmic ray and plasma/field data during the passage of MCs not associated with shock observed during the solar cycle 23&24 (1996-2018); Epoch (zero time) corresponds to start time of MC.

observe (see Fig.2b) that the GCR intensity decrease is small, slowly decreasing with time, and follows the solar wind time profile inversely, as expected during the passage of high-speed solar wind streams from coronal holes [35,36].

A superposed epoch analysis result, with the epoch as the arrival time of MCs not-followed by the high-speed solar wind, is plotted in Fig.2c. From this figure, we notice that such MCs do not produce a large-amplitude, long-lasting decrease in GCR intensity (see Table 1). The effect of such MCs, if any, is very small and transient. It may also be mentioned here that the magnetic field strength in the MC of the two groups is almost equal (see Fig.2b and 2c).These results are consistent with the suggestion that high field magnetically quiet regions (e.g., MCs) are not efficient in the transient modulation of GCR intensity (or producing Forbush decreases) unless they are preceded by the magnetically turbulent structure

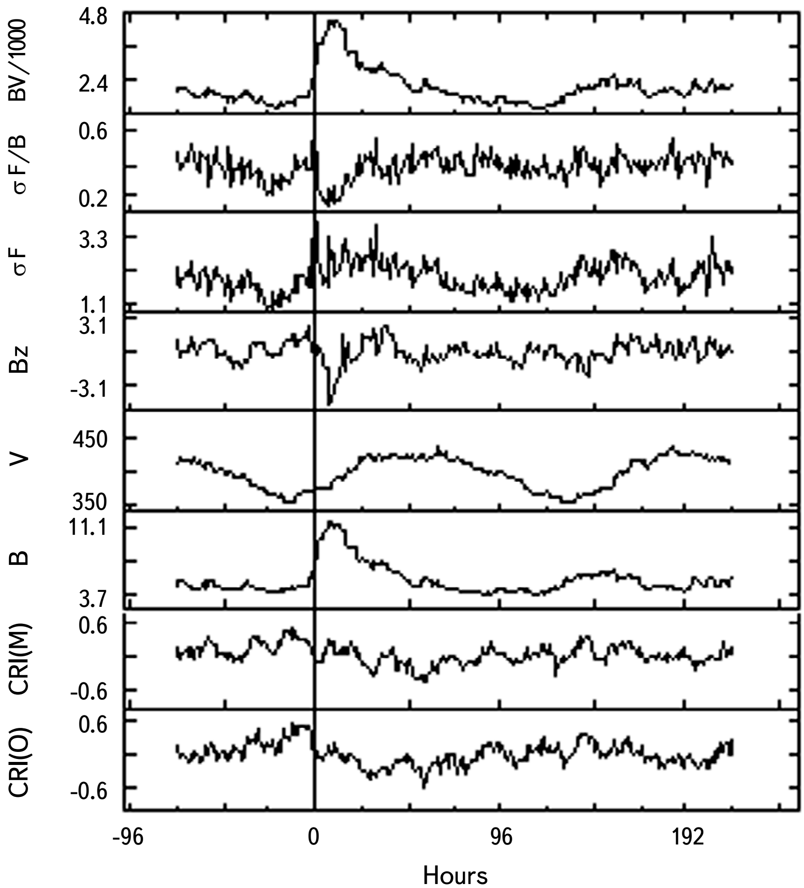

Fig.2b. Superposed epoch analysis results of cosmic ray and plasma/field data during the passage of MCs not associated with shock and followed by high-speed solar wind streams observed during the solar cycle 23&24 (1996-2018); Epoch (zero time) corresponds to start time of MC.

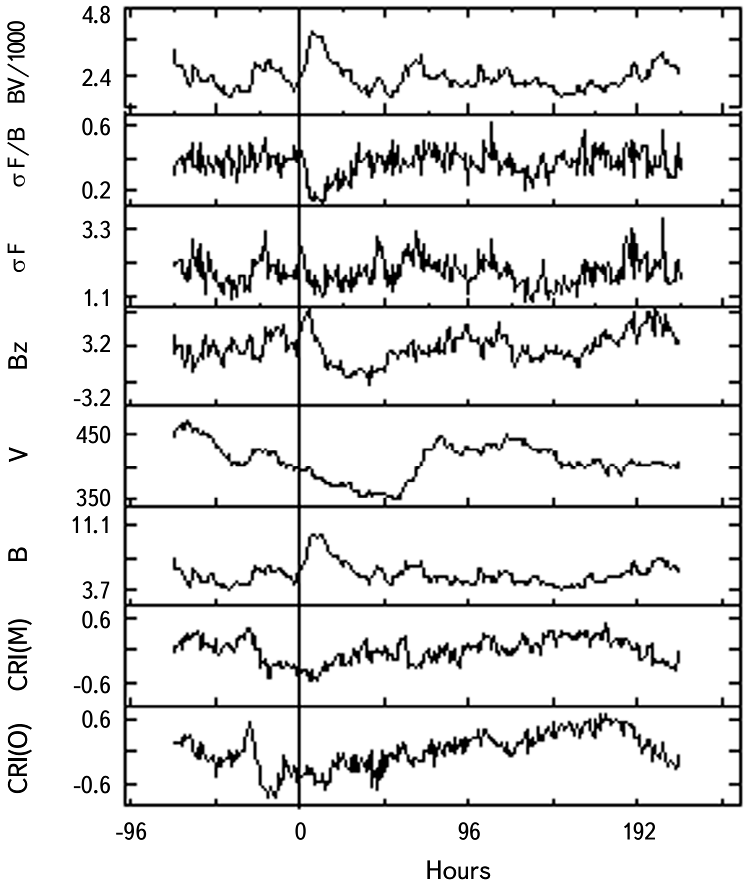

Fig.2c. Superposed epoch analysis results of cosmic ray and plasma/field data during the passage of MCs not associated with shock and not followed by high-speed solar wind streams observed during the solar cycle 23&24 (1996-2018); Epoch (zero time) corresponds to start time of MC.

of shock-sheath regions.

In addition to superposed epoch analysis, we have also applied correlation analysis. In the superposed epoch plots, we notice that during the passage of MCs and their associated structures (e.g., shock, sheath), there is a significant enhancement in solar wind plasma velocity V, interplanetary magnetic field B, and sigma in magnetic field vector σF. Further, these parameters attain a peak value sometime during their passage. We denote these maximum values as V_{max}, B_{max}, and $(\sigma F)_{max}$, respectively. These maximum values are different during the passage of individual MC-associated structures. Moreover, the magnitudes of GCR intensity decreases during the passage of individual MC-associated structures are quite variable [25,32].

Since the maximum speed V_{max}, magnetic field strength B_{max} and/or $(\sigma F)_{max}$

Table 1

THE AVERAGE MAGNITUDE OF CRI DECREASE (%) AND MAXIMUM VALUE OF DIFFERENT PARAMETERS DURING THE PASSAGE OF MCs AND ASSOCIATED STRUCTURES OF SOLAR CYCLE 23&24 OBTAINED FROM THE SUPERPOSED EPOCH PLOTS

S.No.	Structure	[CRI(O)]	[CRI(M)]	$[B]_{max}$	$[V]_{max}$	$[-Bz]_{min}$	$[\sigma F]_{max}$	$[\sigma F/B]_{max}$	$[BV/1000]_{max}$
1	MCs associated with shock	2.050	1.783	14.099	496.491	-2.084	6.340	0.511	7.510
2	MCs not-associated with shock	0.505	0.493	11.118	403.333	-2.002	3.263	0.486	4.288
3	MCs not-associated with shock and followed by HSSWS	0.592	0.623	11.890	404.254	-5.097	3.677	0.523	4.557
4	MCs not-associated with shock and not-followed by HSSWS	0.578	0.339	10.153	396.798	-3.540	2.727	0.448	3.926

of the interplanetary structures are likely to play an important role in transient modulation of GCRs, we utilized these parameters for the correlation analysis with the magnitude of GCR intensity decrease during the passage of MCs and associated structures. Not only these exclusive parameters (V_{max}, B_{max}, $(\sigma F)_{max}$), but a certain combination of these parameters (e.g., $V_{max}B_{max}$, $V_{max}\sigma F_{max}$) have been explored in this correlation study (see Fig.3). Out of these, the parameter that best correlates with the magnitude of transient decrease (Forbush decrease) is $V_{max}B_{max}$ (R = -0.722). A best-fit relationship [CRI (%) = (0.0002299 ± 0.0000174) $V_{max}B_{max}$ + (0.9404 ± 0.23905)], obtained from the linear fit to the data, may be useful in estimating the possible amplitude of transient/Forbush decrease using plasma/field parameters during the passage of magnetic clouds in space.

4. *Conclusions*. From the analysis presented in this paper, we reached the following conclusions:

- During the passage of shock-associated magnetic clouds, the GCR intensity decrease is Forbush-type; it reaches its minimum intensity in two stages of different rate of decrease. In the first stage, which starts at shock arrival, the intensity decreases at a faster rate, with most of the decrease (~85%) happening during this stage within a few hours. This time corresponds to the duration of the sheath region. During the second stage, the intensity decreases at as lower rate. This part is only ~15% of the total decrease, and it happens during the passage of part of the MC. The intensity minimum appears to occur at the central

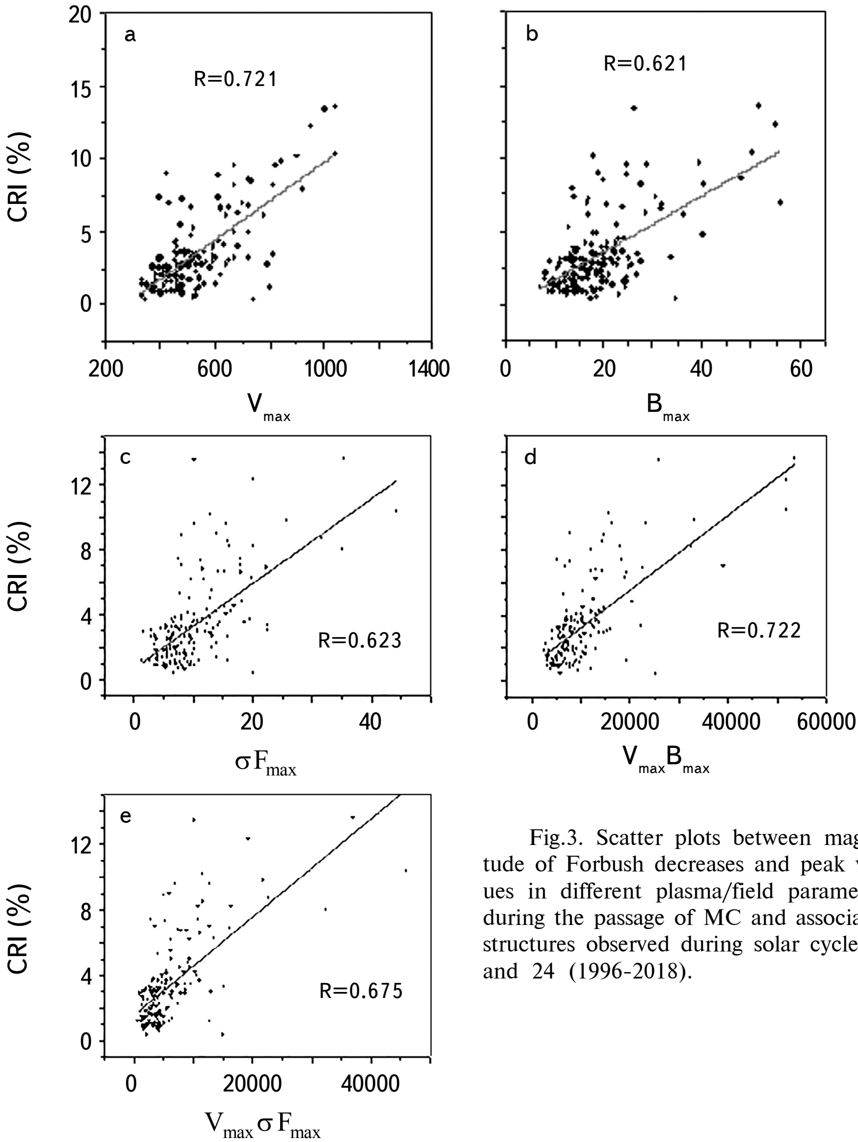

Fig.3. Scatter plots between magnitude of Forbush decreases and peak values in different plasma/field parameters during the passage of MC and associated structures observed during solar cycle 23 and 24 (1996-2018).

axis of the MC. After the passage of the magnetic cloud's central axis, intensity appears to start increasing (recovering) slowly, and this recovery takes a few days' time.

- During the passage of MC, not-associated with shock, and not followed by the high-speed solar wind, a small decrease in GCR intensity may happen only for the duration of MC passage. These MCs appear to be relatively low GCR density regions, and when they cross the point of observation, the detector records a small local decrease in GCR intensity till the passage of the low-density region of MC.

- These results suggest that a high magnetic field region is not an efficient transient modulator of GCRs unless the region is magnetically turbulent also.

- During the passage of MCs, not associated with the shock-sheath region but followed by high-speed solar wind streams, the GCR intensity depresses slowly for a longer time followed by a slow recovery.

- The turbulent sheath region scatters the cosmic ray particles efficiently and is most likely the dominant mechanism for Forbush-type decreases.

- There is some time lag between the minimum GCR intensity and B_{max} as well as σF_{max} during the passage of shock-associated MCs; intensity minimum lags both B_{max} and σF_{max} by a few hours.

- The magnitude of transient GCR intensity decrease due to MC and associated structures is best correlated with a parameter $V_{max}B_{max}$. It shows the importance of the speed of MCs in the GCR intensity modulation. Faster MCs are likely to compress more strongly the preceding ambient plasma and magnetic field ahead of it, resulting in astronger and more fluctuating field in the compressed region of the sheath.

Acknowledgments. We gratefully acknowledge the use of Oulu (https://cosmicrays.oulu.fi/) and Moscow (http://cr0.izmiran.ru/mosc/) neutron monitor data. We thank the station managers of these neutron monitors for making their data accessible. Use of catalogue/data from websites (http://www.srl.caltech.edu/ACE/ASC/DATA/level3/icmetable2.htm), (https://omniweb.gsfc.nasa.gov/form/dx1.html) and (http://spaceweather.izmiran.ru/eng/dbs.html) in this work is also acknowledged with thanks.

Astronomy and Space Science Department, Faculty of Science, King Abdulaziz University, Jeddah, Saudi Arabia, e-mail: badr.physamu@gmail.com

МОДУЛЯЦИЯ ГАЛАКТИЧЕСКИХ КОСМИЧЕСКИХ ЛУЧЕЙ МАГНИТНЫМИ ОБЛАКАМИ И СВЯЗАННЫХ С НИМИ СТРУКТУРАМИ В МЕЖПЛАНЕТНОМ ПРОСТРАНСТВЕ: 1996-2018гг.

М.ФАДААК, Б.БАДРУДДИН

Исследована модуляция галактических космических лучей магнитными облаками, наблюдаемых во время 23 и 24 солнечных циклов (1996-2018гг.).

Использованы данные о плазме и поле солнечного ветра вместе с данными об интенсивности космических лучей во время прохождения магнитных облаков и связанных с ними структур. Применен "наложенный анализ эпох" (superposed epoch analysis) для анализа этих данных. Мы исследовали относительную важность магнитных облаков и связанных с ними структур в модуляции космических лучей. Обнаружены значительные различия в амплитудах и временных профилях транзиентных депрессий в интенсивности космических лучей из-за магнитных режимов при различных напряженностях поля и топологии. Наблюдаемые результаты обсуждены в свете различий в одновременных свойствах плазмы и магнитного поля.

Ключевые слова: *космические лучи:межпланетное пространство:магнитное облако: солнечный ветер:межпланетное магнитное поле*

REFERENCES

1. *L.F.Burlaga*, *E.Sittler*, *F.Mariani et al.*, J. Geophys. Res., **86**, 667, 1981.
2. *R.P.Lepping*, *L.F.Burlaga*, *B.T.Tsurutani et al.*, J. Geophys. Res., **96**, 9425, 1991.
3. *B.Badruddin*, *Y.P.Singh*, Planet. Space Sci., **57**, 31, 2009.
4. *M.V.Alves*, *E.Echer*, *W.D.Gonzalez*, J. Atmos. Sol. Terr. Phys., **73**, 1380, 2011.
5. *O.P.M.Aslam*, *B.Badruddin*, Solar Phys., **292**, 135, 2017.
6. *E.Kilpua*, *H.E.J.Koskinen*, *T.I.Pulkkinen*, Liv. Rev. Solar Phys., **14**, 5, 2017.
7. *B.Badruddin*, *O.P.M.Aslam*, *M.Derouich et al.*, Space Weather, **17**, 487, 2019.
8. *H.V.Cane*, Space Sci. Rev., **93**, 55, 2000.
9. *H.Mavromichalaki*, *A.Papaioannou*, *C.Plainaki et al.*, Adv. Space Res., **47**, 2210, 2011.
10. *K.Kudela*, *R.Brenkus*, J. Atmos. Solar-Terr. Phys., **66**, 1121, 2004.
11. *X.X.Yu*, *H.Lu*, *G.M.Le et al.*, Solar Phys., **263**, 223, 2010.
12. *R.Modzelewska*, *M.V.Alania*, Adv. Space Res., **50**, 716, 2012.
13. *K.P.Arunbabu*, *H.M.Antia*, *S.R.Dugad et al.*, Astron. Astrophys., **580**, A41, 2015.
14. *A.Kumar*, *B.Badruddin*, Solar Phys., **289**, 2177, 2014.
15. *A.Belov*, *A.Abunin*, *M.Abunina et al.*, Solar Phys., **289**, 3949, 2014.
16. *B.Badruddin*, *A.Kumar*, Solar Phys., **291**, 559, 2016.
17. *E.Paouris*, *H.Mavromichalaki*, Solar Phys., **292**, 30, 2017.
18. *M.Dumbovic*, *B.Heber*, *B.Vršnak et al.*, Astrophys. J., **860**, 71, 2018.
19. *A.S.Petukhova*, *I.S.Petukhov*, *S.I.Petukhov*, J. Geophys. Res., **124**, 19, 2019.
20. *A.Papaioannou*, *A.Belov*, *M.Abunina et al.*, Astrophys. J., **890**, 101, 2020.
21. *D.Venkatesan*, *B.Badruddin*, Space Sci. Rev., **52**, 121, 1990.

22. *J.A.Lockwood*, *W.R.Webber*, *H.Debrunner*, J. Geophys. Res., **96**, 11, 587, 1991.
23. *A.Wawrzynczak*, *M.V.Alania*, Adv. Space Res., **45**, 622, 2010.
24. *J.J.Masнas-Meza*, *S.Dasso*, *P.Démoulinet al.*, Astron. Astrophys., **592**, A118 2016.
25. *I.G.Richardson*, *H.V.Cane*, Solar Phys., **270**, 609, 2011.
26. *A.Belov*, *A.Abunin*, *M.Abunina et al.*, Solar Phys., **290**, 1429, 2015.
27. *M.Fadaaq*, *B.Badruddin*, Astrophys. Space Sci., **366**, 10, 2021.
28. *G.Zhang*, *L.F.Burlaga*, J. Geophys. Res., **93**, 2511, 1988.
29. *J.A. Le Roux*, *M.S.Potgieter*, Astron. Astrophys., **243**, 531, 1991.
30. *B.Badruddin*, *R.S.Yadav*, *N.R.Yadav*, Solar Phys., **105**, 413, 1986.
31. *D.V.Reames*, *S.W.Kahler*, *A.J.Tylka*, Astrophys. J. Lett., **700**, L196, 2009.
32. *Y.P.Sigh*, *B.Badruddin*, J. Geophys. Res., **112**, A02101, 2007.
33. *J.Zhang*, *M.W.Leimohn*, *J.U.Kozyra et al.*, J. Geophys. Res., **109**, A09101, 2004.
34. *N.Iucci*, *M.Parisi*, *M.Storini et al.*, Nuovo Cimento, 2C, 421, 1979.
35. *B.Badruddin*, Astrophys. Space Sci., **246**, 171, 1997.
36. *A.Gil*, *R.Iskra*, *R.Modzeleveska et al.*, Adv. Space Res., **35**, 687, 2005.